Enhanced Area Product Method for High-Frequency Inductors and Transformers

Reanna Orzechowski, Matthew Jahnes, Matthias Preindl
Dept. of Electrical Engineering, *Columbia University*, New York, NY USA
Email: reanna.o@columbia.edu, matthias.preindl@columbia.edu

***Abstract*—This paper presents a novel approach to designing magnetics for high frequencies by combining the area product (AP) method with advanced loss modelling techniques. Magnetic components cannot be arbitrarily scaled down at high frequencies due to increased losses as described by the modified AP method for transformer designs to leverage constant loss density under sinusoidal excitation. This study enhances the AP method by incorporating the improved generalized Steinmetz equation (iGSE) and Dowell models to determine the optimal sizing of both transformers and inductors at high switching frequencies. The approach is validated with 2 transformer designs and 2 inductor designs. The experimental results demonstrate the proposed scaling of the transformer designs for a dual-active bridge circuit (DAB) and the inductor designs for a buck converter circuit.**

***Index Terms*—magnetics, loss modelling, Steinmetz, Dowell**

I. Introduction

The design of high-frequency, high-power magnetic components is increasingly important for modern power electronic designs. As modern power electronic switches allow for larger switching frequencies, transformers and inductors must be designed to operate at these larger switching frequencies. The size of an inductor or transformer has widely been determined by the area product method.

Higher switching frequencies may mean smaller magnetic components, but if not designed carefully will also lead to higher magnetic losses due to efficiency and heat limitations. [1] analyzes how the selection of core materials will influence the size of magnetic components for high frequencies. [2] introduces the scaling of transformers considering heat transfer and quality factor limitations. [3] presents a revised AP method to meet constant loss density specifications with sinusoidal excitation using the OSE for core loss estimation and the Dowell model for winding loss estimation. The previous results show roughly 99% efficiency across all 5 transformer designs and a temperature rise between 23-30°C. The experimental results from [3] match closely to the theoretical model and provides a modified AP method for designing transformers with a constant loss density for sinusoidal excitation.

We propose an enhanced AP method for both transformer and inductor designs with constant loss density for any excitation waveform by using the improved generalized Steinmetz equation (iGSE) and the Dowell model. The iGSE was introduced in [4] as a computational tool to more accurately model core losses in magnetic components with any waveform of excitation while still only using the OSE parameters. We will build upon the method outlined in [3] by presenting a method to design high-frequency transformers and inductors for any excitation waveform by combining the iGSE and Dowell model into the AP method.

Many have tried to improve upon the OSE model to provide core loss estimations for non-sinusoidal inputs, leading to the modified Steinmetz equation (MSE), generalized Steinmetz equation (GSE), improved GSE (iGSE) and the improved-improved GSE (i^{2}GSE) [5]–[7]. The MSE, GSE, and iGSE are computationally intense methods but still only rely on the OSE parameters. The i^{2}GSE introduces 5 new parameters in addition to the OSE parameters to also account for the DC bias condition and relaxation effects of magnetics.

While other core loss models exist, we chose to use the iGSE because it is accurate for non-sinusoidal wave-forms without DC bias, it only requires the Steinmetz parameters and it is also easily implemented as a MATLAB function [8], [9]. First we discuss the theory behind core and winding loss estimations including how to incorporate core and winding loss density equations into the original AP method, then we present our chosen inductor and transformer designs, followed by experimental validation and discussion of results.

II. Area Product

As introduced in [10] the product of a transformers window area and cross-sectional core area, A_p is directly related its power requirements by

$$A_p = A_{core}A_{window} = \frac{P_t}{K_f K_u B_m J_w f}, \tag{1}$$

where K_f is a waveform co-efficient, empirically determined as 4.0 for a square wave, K_u is the window utilization factor determined by the winding structure of the copper, P_t is the power handling capability of the transformer, B_m is the peak flux density, J_w is the peak current density, and f is the switching frequency. The volume and weight of a transformer is uniquely determined once its area product is known [3]. Similarly, the area product for an inductor with inductance, L, and RMS current, I_{RMS}, is given as

$$A_p = A_{core}A_{window} = \frac{k_c L I_{rms}^2}{k_w B_m J_w}, \tag{2}$$

where k_c represents the ratio of peak current to RMS current, also known as the crest factor. k_w represents the winding utilization factor. The original AP method assumes a constant magnetic flux density and current density. It is apparent from

(1) and (2) that higher operating frequencies generally mean smaller magnetic components. However, higher switching frequencies come at the cost of higher core and winding loss densities.

III. Methods

A. Winding Loss Modeling

The eddy-current losses in the windings due to the skin and proximity effect are described by the Dowell model [11]. The resistance factor, $F_r(f) = \frac{R_{AC}}{R_{DC}}$ and winding loss density per unit volume of wire with resistivity, ρ, gives the winding loss density as

$$P_w = J_w^2 F_r(f)\rho. \tag{3}$$

The winding of a transformer or inductor can make use of regular copper wire or Litz wire. In the case of regular copper wire, eddy current losses from the skin effect and the proximity effect must be considered. Many modern power electronic designs make use of Litz wire, in which many individual cables are twisted such that each isolated strand occupies every possible position in the wire. While Litz is not a panacea for eliminating winding loss, it reduces skin effect losses compared to traditional round conductors because a single conductors radius within a Litz wire is smaller than its overall skin-depth [12]. The equivalent resistance as a function of frequency for Litz wire was developed in [13] and is given as

$$F_r(f) = \frac{R_{AC}}{R_{DC}} = H + K\left(\frac{ND_i}{D_o}\right)^2 G, \tag{4}$$

$$G = \left(\frac{D_i\sqrt{f}}{10.44}\right)^4, \tag{5}$$

where H is the resistance ratio of individual strands when isolated, G is the eddy-current basis factor, f is the switching frequency, D_i is the diameter of an individual Litz strand, D_o is the outer diameter of the finished cable and K is an empirical constant.

With the resistance factor defined, the winding loss per unit volume of the Litz is then defined in (3). To model a unit winding loss density transformer or inductor with Litz wire, (3) is re-arranged to obtain the following expression for current density,

$$J_w(f) = \sqrt{\frac{P_{winding0}}{F_R(f)\rho}}, \tag{6}$$

where $P_{winding0}$ is a reference winding loss density and F_R is found from (4). This dynamic expression for current density, (6), is then subsituted into AP equation (1) and (2) to yield a magnetic design with a constant winding loss density.

B. Core Loss Modeling

The classic core loss model for sinusoidal excitation is given by the original Steinmetz equation (OSE),

$$P_v = kB_m^\beta f^\alpha, \tag{7}$$

where κ, β, and α are curve-fit parameters, B_m is the peak magnetic flux density at a frequency, f, equating to P_v, the average loss per unit volume.

The iGSE is a core loss model for any excitation waveform using only the original Steinmetz parameters. Further, for excitation waveforms that are piece wise linear with no minor loops, the iGSE has a simple calculation given in terms of the winding voltages, V_j during each time period j of length Δt_j shown in [7] and given as

$$P_v = k_i(\Delta B)^{\beta-\alpha} f \sum_j \left|\frac{V_j}{NA_e}\right|^\alpha (\Delta t_j), \tag{8}$$

$$k_i = \frac{k}{2^{\beta+1}\pi^{\alpha-1}\left(0.2761 + \frac{1}{\alpha+1.354}\right)}. \tag{9}$$

where N is the number of turns, A_e is the cross-sectional area of the core, ΔB is the peak-to-peak flux of the loop under consideration. The constant, k_i employs the OSE parameters and was numerically curve fit to within 0.15% accuracy.

The iGSE equation in (8) is re-arranged to find the peak magnetic flux density versus frequency giving

$$B_m(f) = \frac{1}{2}\left(\frac{P_{v0}}{k_z f}\right)^{\frac{1}{\beta-\alpha}}, \tag{10}$$

$$k_z = k_i \sum_j \left|\frac{V_j}{NA_e}\right|^\alpha (\Delta t_j), \tag{11}$$

where P_{v0} is a reference core loss density chosen by the designer. Assuming symmetry, the peak flux density (B_m) value used in (1) or (2) is assumed to be half of the peak-to-peak value expressed in (8). This is a consequence of assuming there is no DC bias or relaxation effect This dynamic expression for B_m is then substituted into AP equation (1) and (2) to design magnetics for constant core loss density.

IV. Results

A. Analytical Model

The chosen transformer and inductor designs use 3F36 core material which has a saturation flux density of 420 mT at 100°C. Additionally, the designs use AWG 44 Litz wire, consisting of 2625 individual strands twisted together. The design points, chosen somewhat arbitrarily, for the inductor are: a 180 kHz switching frequency, a flux density of 60 mT, and an RMS current of 16 A. The transformer design points are: a 100 kHz switching frequency, a flux density of 350 mT, and a peak current of 30 A. These design points give a reference core and winding loss density, which is then used in the enhanced area product method to size a range of transformer and inductor designs that maintain this constant loss density. Fig. 1 compares the analytical current density and flux density for the enhanced AP, modified AP, and original AP methods. Fig. 2 shows the calculated area product for the enhanced, modified, and original methods.

The enhanced AP method dynamically models the core flux density and winding current density to preserve a constant loss density design for very high switching frequencies. In the case of the 3F36 core material and AWG 44 Litz the AP of the design must be increased at the 100 kHz range. We've also shown that for switching frequencies below 100 kHz, the original AP method suggests a larger design than necessary. The exact switching frequency at which the size must be increased will change depending on the chosen test point and the materials parameters. The test point is a specified switching frequency that achieves a desired test flux density and test current density. The test point will depend on the overall requirements of the converter including the switches and capacitors.

The original AP method assumes a constant magnetizing flux density and constant current density across all switching frequencies. While this assumption could be used with designs that operate below the 100 kHz range, we see higher switching frequencies have different effects. With sinusoidal excitation there is a single harmonic at the operating frequency so the losses are easily extracted with the original Steinmetz equation. Non-sinusoidal wave-forms have higher order harmonics that increase both core and winding losses. If the original AP were to be used for very high switching frequency magnetic designs, we would see saturation and high losses in both the core and the windings.

For the 3F36 material at operating frequencies higher than around 100 kHz (the chosen test point) the volume of the magnetics needs to be increased to preserve a constant loss density. When the input waveform is non-sinusoidal the core loss density is even higher due to higher-order harmonics, requiring magnetics to be increased in size even more than predicted by the modified AP method.

Using the results of the enhanced AP method in Fig. 2, two transformers and two inductors of varying size were built. Photos of the assembled designs are shown in Fig. 3. The corresponding analytical switching frequencies, size, flux density, current density, and efficiency of these designs are shown in Table I.

Transformer design 1 is two EE43/21/20-3F36 cores in parallel. The cores in parallel double the cross-sectional area of the transformer while keeping the window area the same. The effect is that the area product of two EE cores in parallel is double that of a single EE core. Design 2 is a PQ50/50-3F36 core with a much larger window and cross-sectional area due to the nature of the PQ shape, increasing its AP.

Inductor design 1 is two EE42/21/20-3F36 cores with a 6.3 mm air-gap and 12 turns. A variant of inductor design 1 has the same core volume and airgap but has parallel Litz wire and thus 6 turns instead of 12. This design has the same core volume (area product) but now the winding loss density is greatly reduced by using parallel wires.

B. Experimental Validation

A modern transformer application is the dual-active half-bridge circuit. The transformer plays a vital role in this circuit to provide electrical isolation between the primary and secondary sides. The core under test (CUT) shown in Fig. 4a is connected between two half-bridges and connected to the same DC-link. This allows power to circulate from the primary

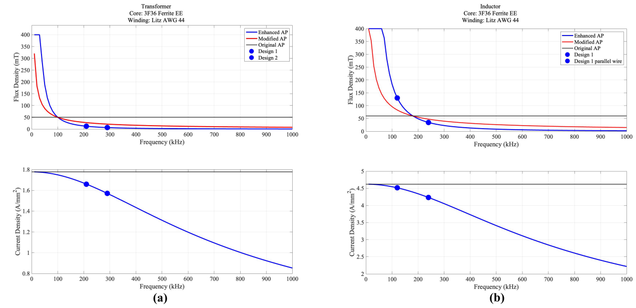

Fig. 1. Comparison of area product design with original AP method, modified AP method and enhanced AP method for (a) transformer and (b) inductor as a function of frequency.

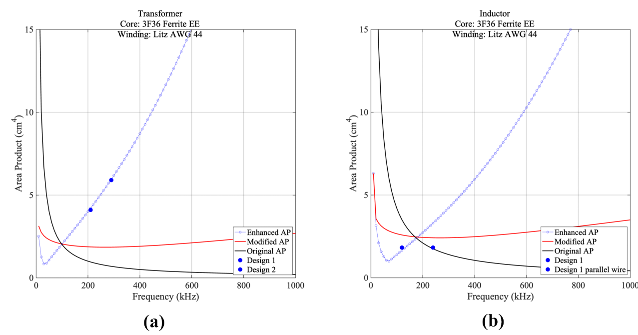

Fig. 2. Comparison of area product design with original AP method, modified AP method and enhanced AP method for (a) transformer and (b) inductor as a function of frequency.

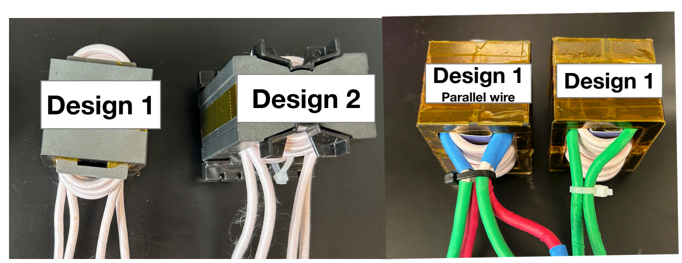

(a) (b)

Fig. 3. Photos of (a) transformer and (b) inductor designs.

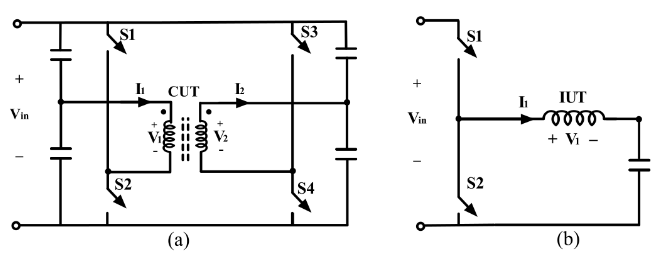

Fig. 4. Experimental set up to measure core losses of (a) transformer and (b) inductor.

TABLE I
ANALYTICAL RESULTS OF MAGNETIC DESIGNS

Transformer					
	F (kHz)	*AP (cm^4)*	B_{m}*(mT)*	J_{w} *(A/mm^2)*	η *(%)*
Design 1	210	4.1	12	1.7	99
Design 2	240	5.9	7	1.6	99

Inductor					
	F (kHz)	*AP (cm^4)*	B_{m}*(mT)*	J_{w}*(A/mm^2)*	η*(%)*
Design 1	120	1.8	187	4.4	98
Design 1 par. wire	240	1.8	187	2.2	99

side of the transformer to the secondary side. The average total loss of the transformer in this configuration is found by taking the difference between the input and output power averaged over one switching period, expressed as

$$P_{loss} = \frac{1}{T}\int_0^T v_2(t)i_2(t) - v_1(t)i_1(t)dt. \tag{12}$$

Similarly when the inductor under test (IUT) is connected to a buck converter circuit as shown in Fig. 4b the average power losses are calculated from the product of the measured current and voltage averaged over one switching period, expressed as,

$$P_{loss} = \frac{1}{T}\int_0^T v_1(t)i_1(t)dt. \tag{13}$$

The transformer designs are tested with a 400 V input voltage, a duty cycle of 0.5 using single-phase-shift (SPS) control in a dual-active half-bridge circuit. As described in [14] the output power of a DAB circuit varies with switching frequency and phase-shift. Each transformer design has a different operating frequency operating point, per its design. To maintain a constant output power of 1kW, the phase-shift is varied accordingly.

The inductor designs are tested with a 400V input voltage and duty cycle of 0.5 in the circuit shown in Fig. 4b. The switching frequency of each design was chosen according to results in Fig. 2.

The input voltage for both the inductor and transformer designs is a PWM signal with fixed duty cycle. The induced current through the transformer and inductor is thus a triangle wave centered around zero.

The goal of the experimental validation approach is to show that each magnetic design has the same efficiency. By measuring the average loss of each design with the same output power, the efficiency is easily extracted.

When measuring loss experimentally, it is important that the probes and equipment are as accurate as possible. It is necessary to ensure that the measurement devices are deskewed so that there is no delay between the voltage and current measurements, which would affect the measured efficiency. It is also essential to ensure that average power is measured over an integer number of switching events.

C. Discussion

Fig. 5 and 6 show the measured voltage and current of the two transformer designs. The difference of the primary and

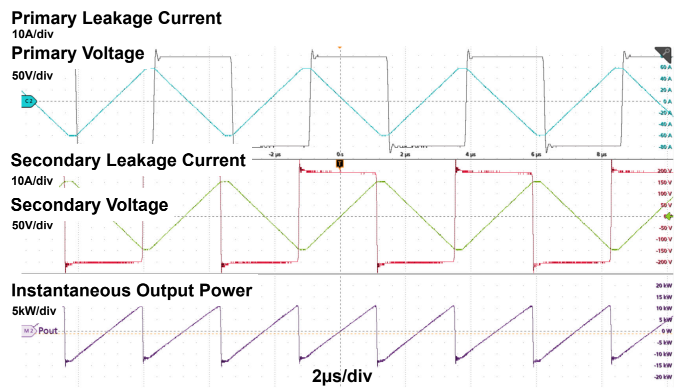

Fig. 5. Experimental results of transformer design 1.

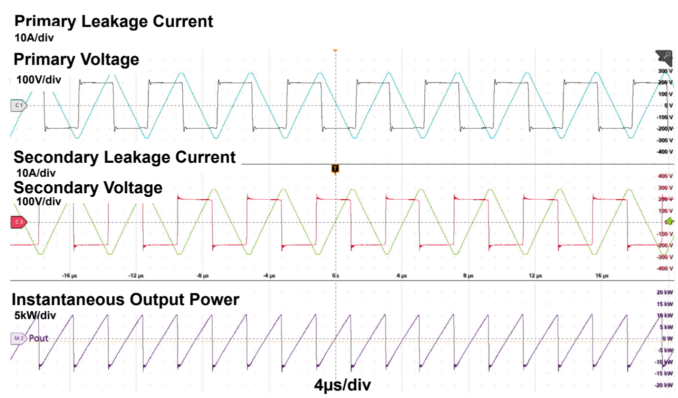

Fig. 6. Experimental results of transformer design 2.

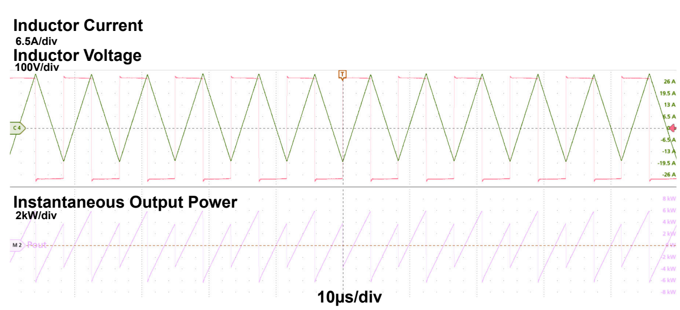

Fig. 7. Experimental results of inductor design 1.

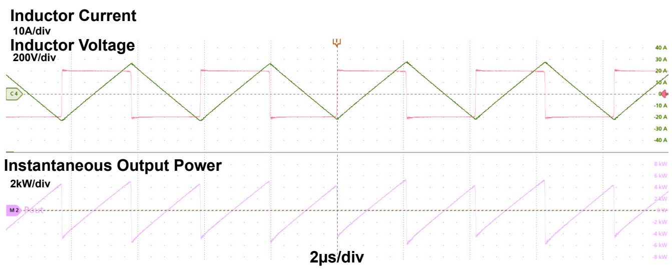

Fig. 8. Experimental results of inductor design 1 with parallel Litz.

secondary side voltage and current is the instantaneous loss. The average loss is the periodic average of the instantaneous loss. The average of the instantaneous output power in conjunction with the average loss is used to calculate the overall efficiency.

Fig. 7 and 8 show the measured voltage and current of the two inductor designs. The instantaneous output power is the product of the measured output voltage and current. The product of the voltage and current through the inductor, gives the instantaneous loss. The efficiency is calculated with the average loss and output power. The results are summarized in Table II

Both transformer designs use the same type of Litz wire, but transformer design 2 has a higher switcher frequency. According to the analytical enhanced AP model, the current density must decrease to maintain constant winding loss density. However, due to the higher switching frequency and the same wire type, the winding loss density is increased. This results in a lower efficiency in transformer design 2. Each design should use a different wire type in order to achieve the desired current density from the analytical model and to maintain a constant loss density. The inductor design with parallel Litz wire results in lower winding loss density. However, there is higher core loss density due to the lower inductance that results from the parallel Litz wire.

These experimental results show that there is an optimum balance between core volume, higher switching frequency, and paralleled wire. We have presented the tools necessary for finding this optimum design based on the requirements of the circuit and of the magnetics, for any excitation waveform.

TABLE II
EXPERIMENTAL RESULTS OF MAGNETIC DESIGNS

Transformer		
	Predicted η (%)	**Measured** η (%)
Design 1	99	96
Design 2	99	86

Inductor		
	Predictedη (%)	**Measured** η(%)
Design 1	98	97
Design 1 par. wire	99	98

V. CONCLUSION

We have introduced an enhanced AP design method by combining the iGSE and the Dowell model to size both transformers and inductors for high switching frequencies with non-sinusoidal excitation. We also demonstrated an experimental validation approach to measure loss density of both inductor and transformers. Future work includes incorporating the relaxation effect into the model. The iGSE does incorporate the relaxation effect into core loss estimation. The i^{2}GSE does incorporate the relaxation effect but requires more parameters than the original Steinmetz coefficients. Future work could show how to improve the core loss accuracy of the magnetic designs in the modified AP equation with the i^{2}GSE.

REFERENCES

[1] David J. Perreault, Jingying Hu, Juan M. Rivas, Yehui Han, Olivia Leitermann, Robert C.N. Pilawa-Podgurski, Anthony Sagneri, and Charles R. Sullivan. Opportunities and challenges in very high frequency power conversion. In *2009 Twenty-Fourth Annual IEEE Applied Power Electronics Conference and Exposition*, pages 1–14, 2009.

[2] M.G. Odendaal and J.A. Ferreira. Effects of scaling high frequency transformer parameters. In *IAS '97. Conference Record of the 1997 IEEE Industry Applications Conference Thirty-Second IAS Annual Meeting*, volume 2, pages 1123–1130 vol.2, 1997.

[3] W.-J. Gu and R. Liu. A study of volume and weight vs. frequency for high-frequency transformers. In *Proceedings of IEEE Power Electronics Specialist Conference - PESC '93*, pages 1123–1129, 1993.

[4] K. Venkatachalam, C.R. Sullivan, T. Abdallah, and H. Tacca. Accurate prediction of ferrite core loss with nonsinusoidal waveforms using only steinmetz parameters. In *2002 IEEE Workshop on Computers in Power Electronics, 2002. Proceedings.*, pages 36–41, 2002.

[5] J. Reinert, A. Brockmeyer, and R.W.A.A. De Doncker. Calculation of losses in ferro- and ferrimagnetic materials based on the modified steinmetz equation. *IEEE Transactions on Industry Applications*, 37(4):1055–1061, 2001.

[6] Jieli Li, T. Abdallah, and C.R. Sullivan. Improved calculation of core loss with nonsinusoidal waveforms. In *Conference Record of the 2001 IEEE Industry Applications Conference. 36th IAS Annual Meeting (Cat. No.01CH37248)*, volume 4, pages 2203–2210 vol.4, 2001.

[7] J. Mühlethaler, J. Biela, J. W. Kolar, and A. Ecklebe. Improved core loss calculation for magnetic components employed in power electronic system. In *2011 Twenty-Sixth Annual IEEE Applied Power Electronics Conference and Exposition (APEC)*, pages 1729–1736, 2011.

[8] yoash levron. magnetic core loss for arbitrary flux waveforms. https://www.mathworks.com/matlabcentral/fileexchange/39995-magnetic-core-loss-evaluation-for-arbitrary-flux-waveforms, 2023. [MATLAB Central File Exchange; Retrieved June 29, 2023].

[9] J.Czogalla C.Sullivan, K. Venkatachalam. Caclulate power loss in a ferrite core. http://inductor.thayerschool.org/coreloss.shtml, 2003. [Dartmouth Magnetic Component and Power Electronic Research; Retrieved June 29, 2023].

[10] C. T. McLyman. Transformer and inductor design handbook. In *Kg Magnetics*, 2004.

[11] P.L. Dowell. Effects of eddy currents in transformer windings. In *Proceedings of the Institution of Electrical Engineers*, volume 113, pages 1387–1394, 1966.

[12] Zhuoyuan Liu, Jianguo Zhu, and Lihua Zhu. Accurate calculation of eddy current loss in litz-wired high-frequency transformer windings. *IEEE Transactions on Magnetics*, 54(11):1–5, 2018.

[13] F.E. Terman. Radio engineers' handbook. In *McGraw-Hill Book Company*, page 30–83, 1943.

[14] Shuntaro Inoue, Masanori Ishigaki, Atsuhiro Takahashi, and Takahide Sugiyama. Design of an isolated bidirectional dc–dc converter with built-in filters for high power density. *IEEE Transactions on Power Electronics*, 36(1):739–750, 2021.